Tip-Induced Nanostructuring of a Clean and Ethene-Modified Pt(111) Electrode with Cu

Peter Berenz, Xiaoyin Xiao, and Helmut Baltruschat*

Institut für Physikalische und Theoretische Chemie, Römerstr. 164, D-53117 Bonn, Germany

Received: August 7, 2001

The adlayer formed when ethene is adsorbed from sulfuric acid solution on a Pt(111) electrode at room temperature has a disordered structure. Small domains with local ordering are discernible by STM. The adsorbate is not (or only to a minor extent) displaced by Cu−UPD. Scanning the surface in a very small area with the tip very closely approached to the surface leads to displacement of the organic adsorbate followed by Cu−UPD. Scanning under similar conditions over the surface free of the organic adsorbate, but covered by UPD−Cu also leads to a nanostructuring of the surface. Structures of sizes down to 5 nm can be fabricated by this kind of nanolithography. The results are interpreted by a local, tip-induced alloy formation.

Introduction

From the early stages of scanning tunneling microscopy on, it was an aim not only to investigate surfaces but also to use the STM as a tool for nanostructuring. Of particular interest are those approaches which work under ambient pressure and temperature, i.e., in most cases approaches using electrode surfaces.

Lebreton et al.[1] were able to make a stable nanohole (3 nm large, one monatomic layer deep) on a gold film with (111) surface using the tip of a scanning tunneling microscope (STM) and studied the mechanism of this nanohole formation. A linear relationship between the hole area and the pulse duration was observed, suggesting an anodic oxidation process of the gold surface under a voltage pulse and a place-exchange mechanism, involving the lifting of gold atoms in the surface monolayer, are relevant in nanohole formation.

Park et al.[2,3] used the STM tip as nanoscale tweezers. Self-organized Ag nanoclusters on a Sb modified Si(100) surface could be selectively detached and manipulated at room temperature by proper adjustment of the electrical field at the tip.

Kolb and co-workers[4−8] used the tip of the STM to deposit nanometer-sized clusters of copper or silver on bare and thiol-covered gold electrode surfaces. After electrochemical metal deposition onto the STM tip, the clusters are formed by a jump-to-contact between the tip and the substrate during a short and very controlled approach of the tip toward the surface. Ni deposited onto the tip turns the jump-to-contact into the opposite direction, leaving holes in the gold surface. The stability of the metal clusters against anodic dissolution is astonishing.

Another procedure has been described by Schindler et al.[9,10] for localized electrochemical deposition of small Co clusters on Au(111) by using the STM tip as an electrochemical nanoelectrode. In this approach, Co is first accumulated on the tip and then dissolved from the tip; the high concentration underneath the tip leads to deposition of Co clusters on the substrate with diameters down to 15 nm. The locally higher concentration in the electrolyte leads to a preferential deposition in the vicinity of the tip, provided that the electrode potential is appropriately chosen.

Small Ag particles with a diameter of 20−40 nm were locally deposited on HOPG in a process involving the introduction of defects on the substrate (ref 11 and references therein). Surface defects introduced by the tip were probably also responsible for the local enhancement of Cu growth rate on a Cu substrate introduced by the tip−sample force.[12,13] The authors show the general applicability of this scheme on Au(111) passivated with self-assembled octadecanethiol monolayers.[12,13]

The possibility of a local tip-induced dissolution of Cu from an electrode at potentials at which Cu dissolution should normally not occur was demonstrated by Kolb and co-workers.[14] The dissolution process took place only underneath the tip allowing for a nanometer scale patterning of the Cu surface. The authors offered an explanation for the tip-induced metal dissolution on the basis of a direct charge transfer to the tip. This technique can also be used for the local dissolution of Cu clusters on Pt and is able to reveal the atomic structure of the lowest deposited layers.[15]

Chi et al.[16] also created nanoscale pits but in a slightly different method. They fabricated nanoscale pits on Au(111) in aqueous environments by in-situ STM, on the basis of critical interactions between tip and substrate. The authors characterized parameters affecting the pit formation and size systematically showing that pit formation is dominated by bias voltage and propose a mechanism based on local surface reconstruction induced by electronic contact between tip and substrate. This proposal deviates from the mechanism suggested by Kolb.[14]

Ertl and co-workers[17] report that the application of ultra short voltage pulses between a 10 μm thick wire electrode and a work piece in an electrochemical environment allowed the three-dimensional machining of conducting materials with submicrometer precision. The principle is based on the finite time constant for double-layer charging, which varies linearly with the local separation between the electrodes. This technique was used for local etching of copper and silicon as well as for local copper deposition. The structures made by this method are of course in the range of micrometers.

Liu et al.[18] used the AFM to fabricate either holes in thiol self-assembled monolayers on Au ("nanoshaving") or to create nanostructures with longer chain lengths ("nanografting"). Most of these methods have been shown to work for soft substrates.

When starting this work, it was our goal to use adsorbed ethene as a mask for Cu deposition: it was our intention to locally scratch away the organic adsorbate with the tip and thus

* To whom correspondence should be addressed.

10.1021/jp013070g CCC: $22.00
Published on Web 03/19/2002

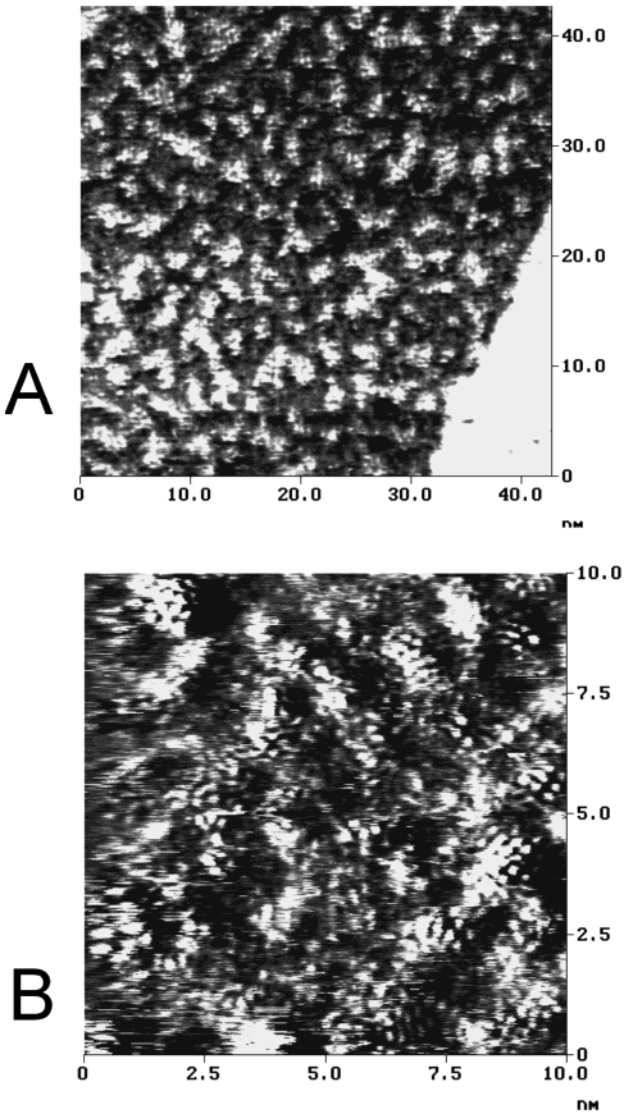

Figure 1. In situ STM images after adsorption of ethene on a Pt(111) electrode surface from ethene saturated 0.05 M H_2SO_4 solution and after electrolyte exchange to pure 0.05 M H_2SO_4 at 100 mV vs Cu/Cu^{2+}. (A) obtained in constant current mode, $U_{bias} = 35$ mV, $I_{tip} = 2$ nA. (B) Obtained in constant height mode, $U_{bias} = 10$ mV, $I_{tip} = 24$ nA.

to achieve a local deposition of Cu. It then turned out that the same nanostructuring is also possible in the absence of ethene. However, for a subsequent deposition of further metallic layers onto the primary nanostructure (which is not the topic of this work), such a "mask" is necessary. The results obtained on ethylene-covered surfaces will therefore also be described here.

A large number of studies on the adsorption of ethene on metal surfaces in UHV can be found in the literature, e.g., refs 19−22. In short, ethene is adsorbed at low potentials as a π-bound or di-σ-bound species and undergoes a transition to ethylidyne (or similar species) at room temperature. Two reports used scanning tunneling microscopy to study the adsorption of ethene on Pt surfaces. Ethylidyne formed by adsorbing ethene on Pt(111) and annealing to 350 K under UHV conditions can only be depicted by STM at low temperature (180 K). It was argued that at room temperature the STM images are blurred because of the low-frequency vibrations.[23]

Ronning et al.[24] investigated the adsorption and subsequent dehydrogenation of ethene on the hexagonally reconstructed Pt-(100)-hex-R0.7° surface using scanning tunneling microscopy

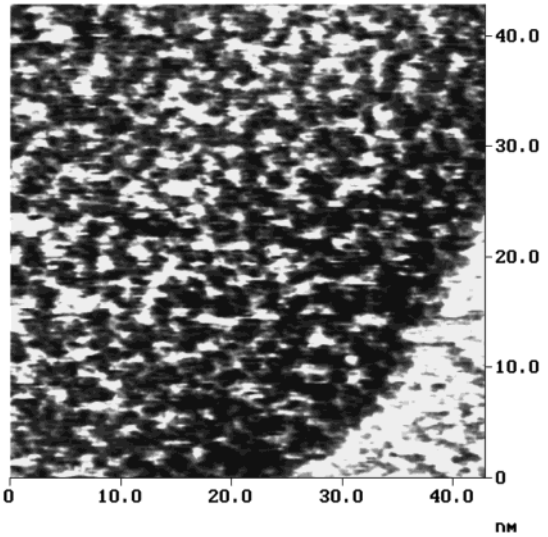

Figure 2. In situ STM image after adsorption of ethene on a Pt(111) electrode surface and after electrolyte exchange from ethene saturated 0.05 M H_2SO_4 solution to 4×10^{-4} M $CuSO_4$ + 0.05 M H_2SO_4 solution at 100 mV vs Cu/Cu^{2+}. $U_{bias} = 50$ mV, $I_{tip} = 1$ nA.

and low energy electron diffraction (LEED). Their results confirm that heterogeneous nucleation of the (1 × 1) domains occurs when the hexagonal reconstruction is lifted during ethene adsorption on Pt(100).

On Pt electrode surfaces, we have shown by differential electrochemical mass spectrometry (DEMS)[25] that a variety of adsorbate states exists,[26,27] which we are tempted to assign to those identified on Pt surfaces in UHV. In particular, on both polycrystalline Pt and Pt(111) electrodes, we have found that only around 10% of the adsorbed ethene is displaced by Cu^{2+} ions from solution at potentials close to the Nernst potential of Cu when a Cu UPD layer is formed on clean Pt surfaces.[28] Adsorbed benzene, on the contrary, is completely displaced by Cu UPD.

Experimental Section

The STM imaging was performed with an STM head from Molecular Imaging and a Nanoscope E controller from Digital Instruments. All STM measurements were done at room temperature in constant current mode. The Pt/Ir (90:10) tips were etched in KSCN + KOH solution and coated with anodic electrophoretic paint to reduce the area in contact with the electrolyte. A Pt wire was used as the counter electrode. As a reference electrode, a Cu wire was immersed in the same solution, separated from the STM cell by a glass frit. The STM cell was maintained under an argon atmosphere. The bias voltage U_{bias} is the tip potential minus working electrode potential.

Electrolytes were prepared from sulfuric acid (Merck, p.a.), cupric sulfate pentahydrate (Fluka, p.a.), and Milli-Q water (Millipore). The working electrode was a Pt(111) single-crystal oriented within an accuracy of 0.5°, obtained from Metal Crystals & Oxides. The preparation of the single crystal was done by flame annealing. The cooling was performed in an H-cell over Milli-Q water in a 5 N argon atmosphere. Preparation quality and cleanliness were checked first in a conventional H-cell and then in the STM cell with 0.05 M H_2SO_4 by cyclic voltammetry. Then the pure sulfuric acid was replaced under potential control at 0.1 V (vs Cu/Cu^{2+}) by 4×10^{-4} M Cu^{2+} ions containing sulfuric acid solution or, in the experiments involving ethene, by ethene saturated sulfuric acid. After

adsorbing ethene for 4 min, the solution was then replaced by pure sulfuric acid or by the Cu^{2+} ion containing solution.

Results

An STM image of ethene adsorbed at a Pt (111) electrode under pure 0.05 M H_2SO_4 at 0.1 V vs Cu/Cu^{2+} is shown in Figure 1. No well-ordered adlayer is visible. Instead, very small domains with a local ordering of around 10 height maxima are observed. The height maxima in these domains may be due to ethene (or ethylidyne) molecules. In an alternative interpretation, these height maxima would be ascribed to the substrate atoms, because their separation of ~0.3 nm is close to the lattice constant of the substrate. The blurred regions between would then be due to the isolation effect of disordered ethene. However, a Fourier transform of the whole image did not indicate any long range order. This should be the case if the height maxima were due to the substrate atoms and, therefore, a phase correlation of the various domains existed. (Also, the seemingly rectangular structure contradicts such an interpretation.) We therefore believe that the height maxima really correspond to any of the adsorbed ethene species (e.g., ethylidyne).

The structure observed for ethylidyne in UHV at low temperatures[23] also looks somewhat disordered although a local order is discernible. However, the distance between the maxima (i.e., the ethylidyne molecules) in UHV is twice that of the substrate lattice constant. A further difference is that our images were obtained at room temperature. This last effect might be ascribed to the presence of water or to the influence of the electrode potential. However, using DEMS, we have identified the presence of several adsorbate states, which we were tempted to ascribe to π-bound ethene and di-σ-bound ethene (which can both be desorbed under hydrogenation to ethane), ethylidyne, and an oxygen containing adsorbate. Therefore, the locally ordered domains at the electrode surface may also be due to flat lying ethene (which in UHV is no more stable at room temperature) or to the oxygenated species. The blurred regions between the small ordered domains might then be due to ethylidyne.

An identical structure was observed when after ethene adsorption the electrolyte was exchanged by 4×10^{-4} M Cu^{2+} in 0.05 M H_2SO_4 (Figure 2). The similarity of the images shows that no drastic change had occurred in the surface structure and

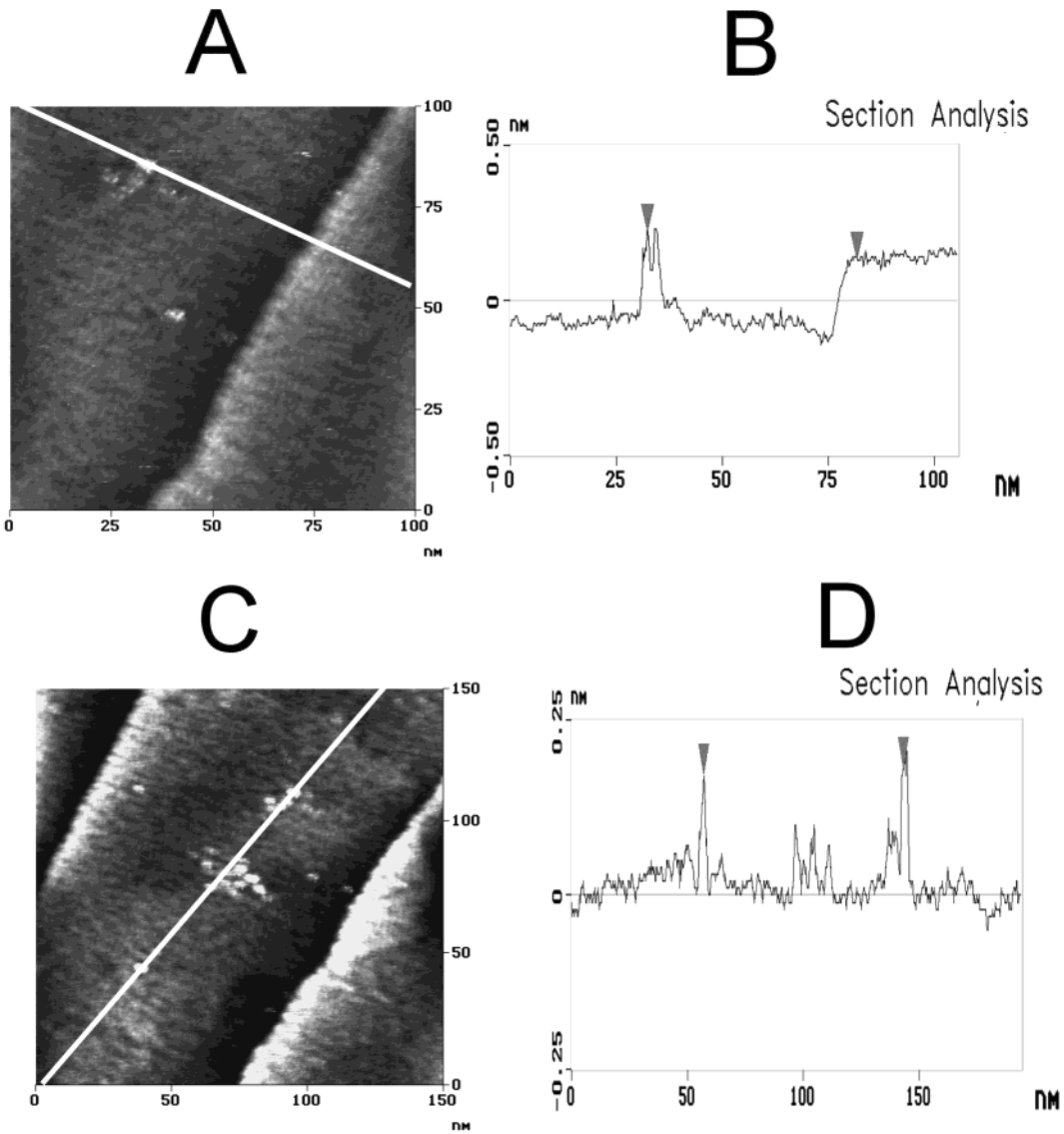

Figure 3. In situ STM images of several nanoclusters artificially deposited onto ethene covered Pt(111) electrode surface (A and C) and section analysis (B and D). $U_{bias} = 50$ mV, $I_{tip} = 1$ nA. Manufacturing conditions: $E_w = 100$ mV vs Cu/Cu^{2+}, $U_{bias} = +2$ mV, $I_{tip} = 20$ nA. Tip velocity, 720 nm/s; scanned area, 10 nm × 10 nm; total scanning time, 0.5 min per cluster.

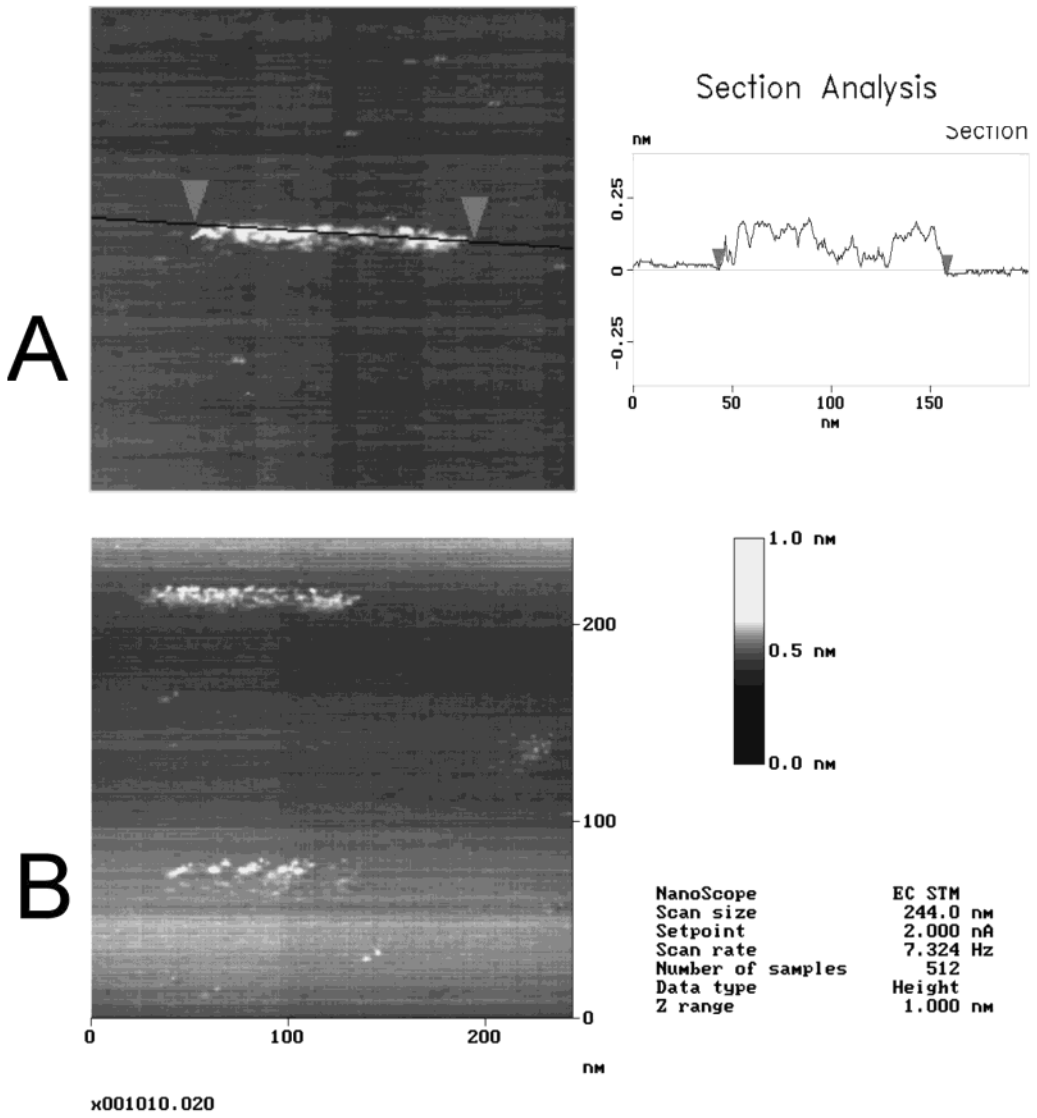

Figure 4. Tip-induced nanostructure stripes on to a Cu UPD covered Pt(111) surface in 0.05 M H_2SO_4 /10^{-4} M $CuSO_4$. Manufacturing conditions: E_w = 100 mV vs Cu/Cu^{2+}, U_{bias} = −2 mV, I_{tip} = 20 nA, Tip velocity, 7200 nm/s; scanned area, 100 nm × 7 nm; total scanning time, 1 min. Imaging conditions: E_w = 100 mV vs Cu/Cu^{2+}, U_{bias} = −20 mV, I_{tip} = 2 nA. (A) first manufactured stripe and section analysis. (B) Larger scan area after setting a second stripe in parallel.

composition, confirming our previous DEMS data that ethene is displaced by Cu UPD only to a minor extent.[29]

In a series of experiments, we induced desorption of the adsorbate accompanied by underpotential deposition of Cu by scanning with the tip very close to the surface at the potential positive of the Nernst potential (E_w = 100 mV vs Cu/Cu^{2+}; U_{bias} = 2 mV, I_{tip} = 30 nA) with a scan range of 10 nm × 10 nm. Several spots close to each other were thus generated. The subsequent image, obtained under usual tunneling parameters (U_{bias} = 50 mV, I_{tip} = 1 nA), shows that a 2D cluster with a diameter of ∼5 nm and of monatomic height had thus been made (Figure 3A,B). After depositing several such clusters into separate groups in the same region, a further single cluster was then deposited on a connecting line of the two groups of clusters (Figure 3C,D).This indicates again that structures of down to 5 nm can be fabricated in this way.

In another set of experiments, the tip was scanned in an area of 100 nm × 7 nm for 1 min on a copper UPD covered Pt(111) surface in copper solution without using any organic adsorbate. The tunneling parameters were set to I_{tip} = 20 nA and U_{bias} = −2 mV at a potential of 100 mV vs Cu/Cu^{2+}. Somewhat unexpected, the STM image obtained subsequently at a larger surface to tip distance (Figure 4) also shows the formation of nanostructured line. The line width is only 9 nm so that there is a difference of only 2 nm of set and done width. A cross section shows that the structures are monatomic high (0.2 nm). However, the line is not completely flat: there are some missing areas (Figure 4). In control experiments without Cu^{2+} ions in solution, we never observed the formation of such structures.

Similar stripes were drawn in the presence of the ethene adlayer with different scan angles. In Figure 5, such structures are shown, which have a size of 108 nm × 18 nm, which is only 4 nm more than the set width value. The smaller stripe in the center of the figure seems to be caused by a double tip effect during the deposition process. As can be seen from both the cross section and the height distribution analysis of one of the stripes in Figure 5b, the average height of the structure on the ethene covered surface is 0.3 nm. To determine the influence of the scanning time, we produced the structures shown in Figure 6. Here, the time of the tunneling under these severe tunneling conditions was about 5 times larger than in the previous image. The cluster at the step, which is marked as "5" and probably due to a contamination, was used as a marker. Four clusters were deposited at the corners of a parallelogram. Because of

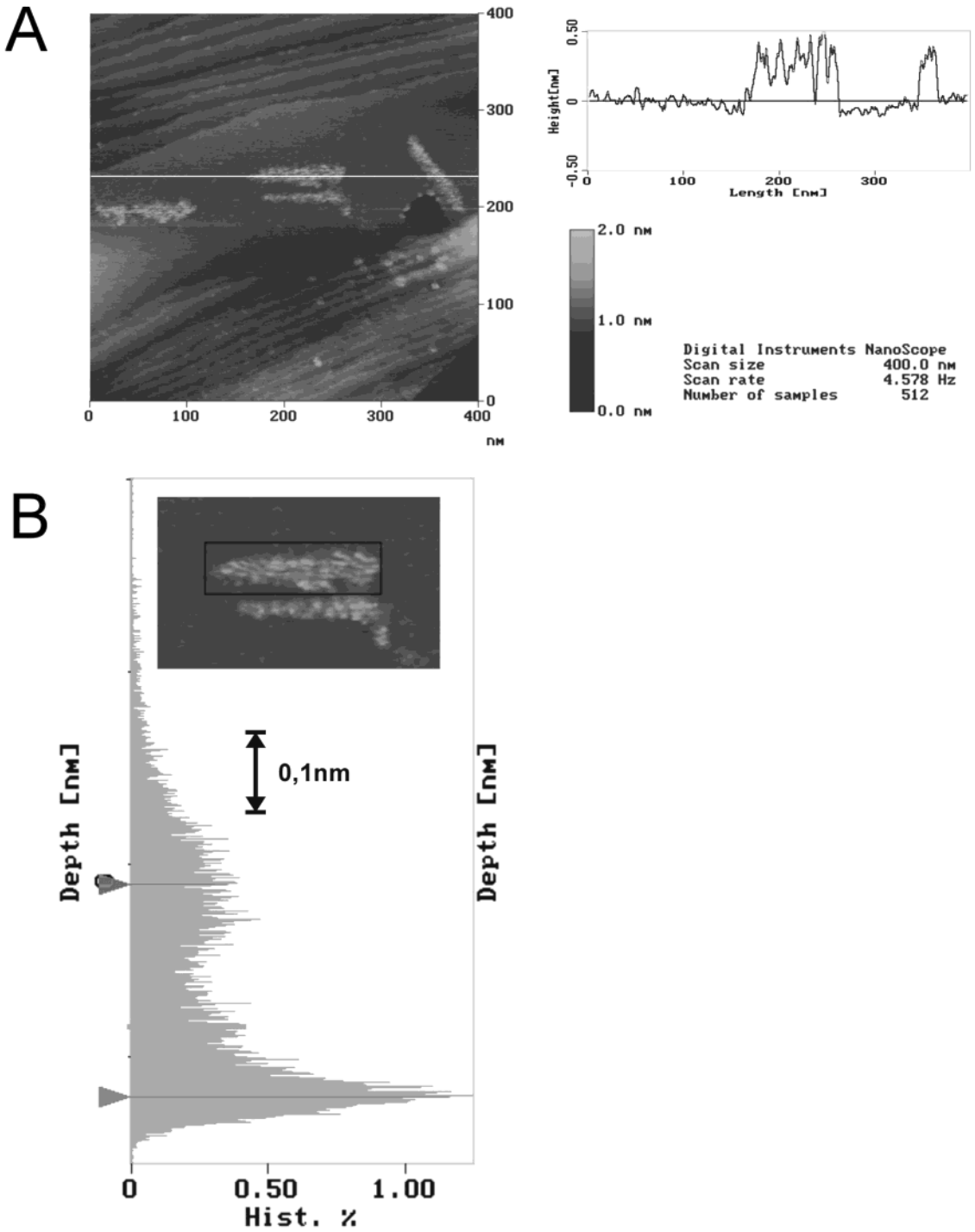

Figure 5. Tip-induced nanostructure stripes on an ethene covered Pt(111) surface in 0.05 M H_2SO_4 /10^{-4} M $CuSO_4$. Manufacturing conditions: $E_w = 100$ mV vs Cu/Cu^{2+}, $U_{bias} = +2$ mV, $I_{tip} = 20$ nA. Tip velocity, 7200 nm/s; scanned area, 100 nm × 12 nm (horizontal stripes); total scanning time, 1 min/stripe. Imaging conditions: $E_w = 100$ mV vs Cu/Cu^{2+}, $U_{bias} = +20$ mV, $I_{tip} = 1$ nA. (A) Image of all manufactured structures with section analysis. (B) Depth histogram of the second placed stripe.

the longer scanning time, their height is now about 1 nm. After the potential was increased to 250 mV vs Cu/Cu^{2+}, only the smallest cluster was dissolved, confirming that the clusters do not consist of bulk Cu but rather of an alloy.

To investigate the influence of organic layers on height differences of these structures, a separate experiment with silver UPD and adsorbed ethene was performed: a monolayer of silver was deposited at the open circuit following the procedure of Clavilier[30] before introducing the crystal into the STM cell. In the STM cell, roughly 50% of this Ag was dissolved, and then ethene was adsorbed on to the blank Pt areas. We suppose that the bright areas in Figure 7 are due to monatomic high Ag islands. The darker areas should be the ethene-covered Pt surface. The bright spots within the dark areas correspond to the small domains of ethene in Figures 1 and 2. The height difference between these areas is around 0.1 nm.

Discussion

Because the clusters are deposited at potentials positive of the Nernst equilibrium potential, they cannot consist of bulk Cu. This is further demonstrated by the high stability of the clusters even after a potential step to +250 mV positive of the

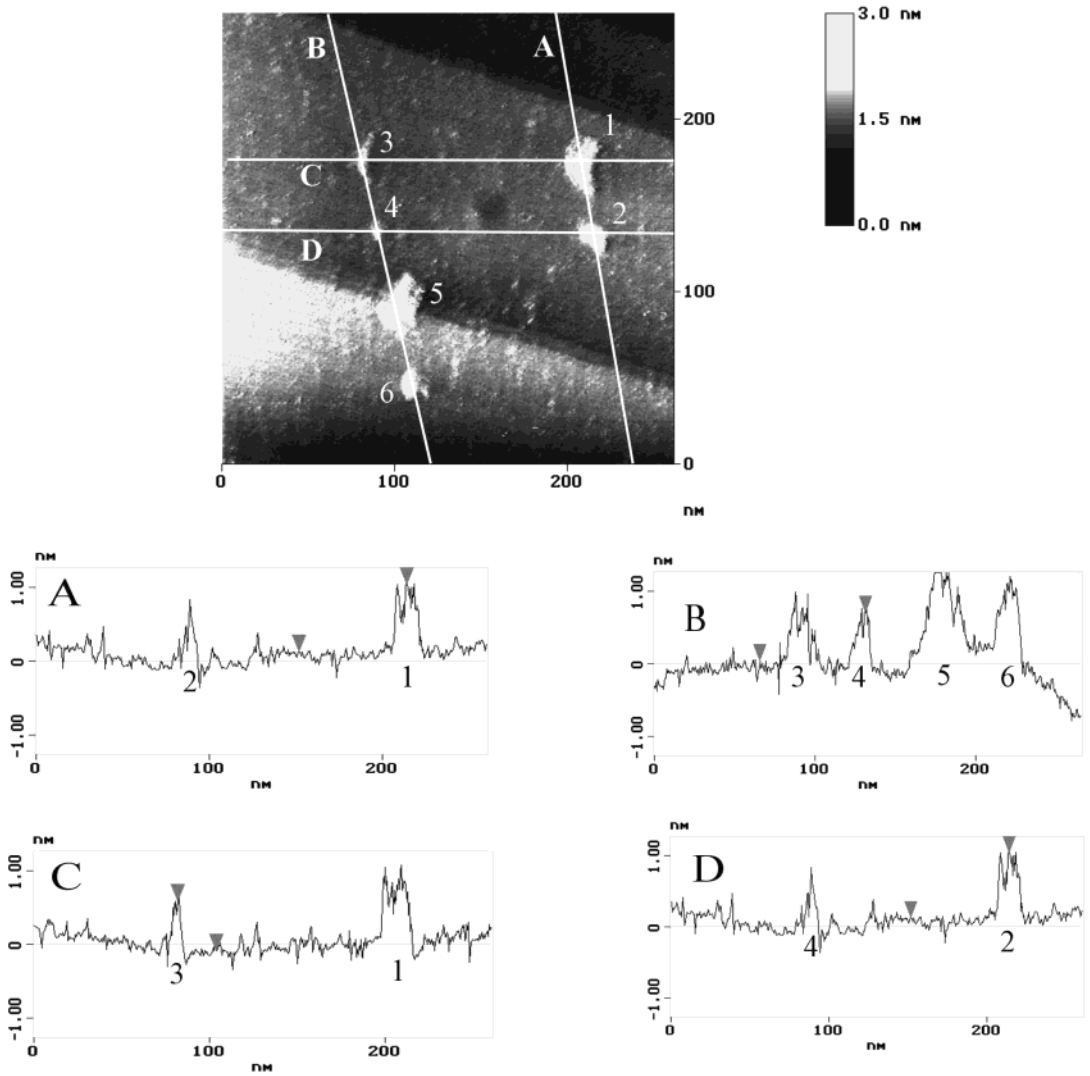

Figure 6. Section analysis of four tip-induced nanoclusters on an ethene covered Pt(111) surface in 0.05 M H_2SO_4 /10^{-4} M $CuSO_4$. Manufacturing conditions: $E_w = 74$ mV vs Cu/Cu^{2+}, $U_{bias} = +2$ mV, $I_{tip} = 20$ nA. Tip velocity, 720 nm/s; scanned area, 10 nm × 10 nm; total scanning time, 5 min. Imaging conditions: $E_w = -18$ mV vs Cu/Cu^{2+}, $U_{bias} = +100$ mV, $I_{tip} = 1$ nA. The highest cluster is 1 nm high. The two clusters on the upper terrace (at the bottom of the image and the edge of the double step) are caused by impurity of the surface, not by our tip.

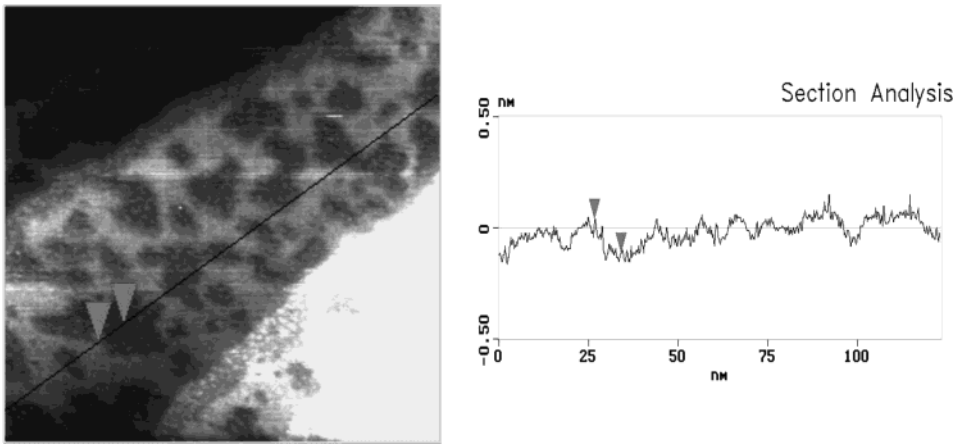

Figure 7. Pt(111) surface covered by 45% silver UPD (bright area) and ethene (dark area) in 0.05 M H_2SO_4 /10^{-4} M $CuSO_4$. Imaging conditions: $E_w = 100$ mV vs Cu/Cu^{2+}, $U_{bias} = +50$ mV, $I_{tip} = 1$ nA, 100 nm × 100 nm. The section analysis shows a height difference between the Ag UPD and the ethene layer of 0.1 nm.

equilibrium potential. The structures produced are neither just a monolayer, because they are not only too high, but also formed on a surface already covered by a monolayer of Cu (cf. Figure 4). We therefore conclude that this kind of nanostructuring is due to the localized formation of an alloy. This alloying is probably caused by a force interaction between the tip and the surface, leading to an atomic place exchange by direct impact between the atoms.

Alternatively, one might think of a local temperature increase as being the origin of the local alloying. However, a simple

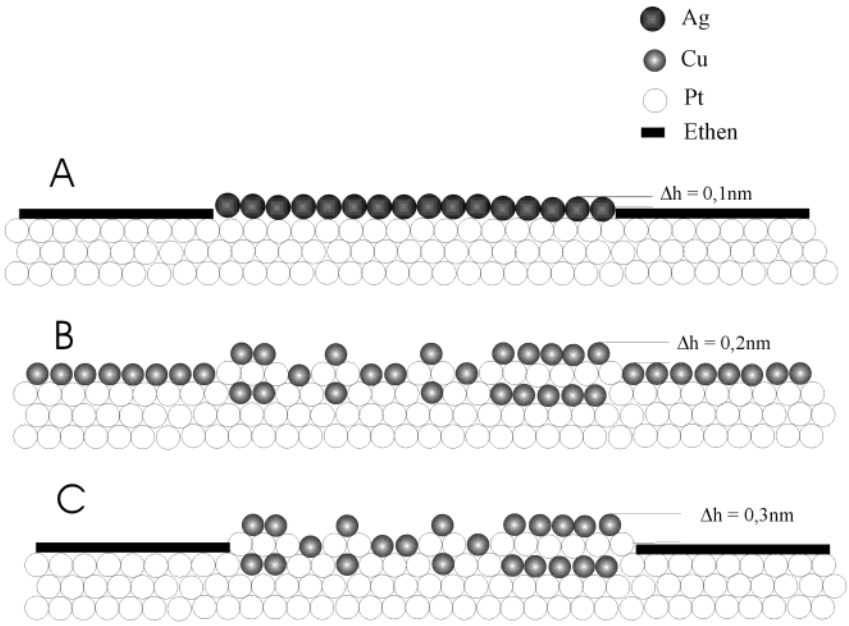

Figure 8. Schematic models of the manufactured structures. (A) Silver UPD with neighboring ethene on platinum, the height difference between Ag and ethene is 0.1−0.16 nm. (B) Tip-induced Pt/Cu alloy made from Cu UPD covered Pt surface, the height difference here is 0.2 nm. (C) Tip-induced Pt/Cu alloy made from ethene covered Pt surface in copper ions containing electrolyte at UPD potential region, the height difference here is 0.3 nm.

estimation shows that this cannot be the case. Such a temperature increase could be caused by electric heating or by the friction. For a bias voltage of 2 mV and a tunneling current of 20 nA, the electric power is 40×10^{-12} W. When a relatively high lateral friction force of 10 μN, which is just below the value for scratching silicon surfaces,[31] and a path length per second of 10 nm $\times$ 36 s^{-1} are assumed, the heat produced because of friction is 3.6×10^{-12} W. An estimation of the temperature increase ΔT can be made assuming stationary, spherical heat conductance. According to $dQ/dt = \lambda ADT/r_0$, where Q is the heat, A is the surface area of 10 nm $\times$ 10 nm, r_0 is an assumed radius of 5 nm, and λ is the heat conductance (0.71 J s^{-1} cm^{-1} K^{-1} for Pt), a temperature increase of only $\Delta T = 3 \times 10^{-5}$ K is calculated, which certainly is negligible. Thus, a direct atomic impact seems to be the origin of the alloying. A corresponding model of the structures and the influence of the ethene adsorbate on height differences is shown in Figure 8.

Because ethylene is not strongly adsorbed at Ag electrodes (there are neither any reports on its adsorption nor does ethene adsorb at Ag surfaces in UHV at room temperature), the measured height difference in the experiment of Figure 7 corresponds to an ethene-covered Pt and a free Ag UPD surface. The experimental height difference of ~0.1 nm is due to the difference in the effective thickness of the ethene layer and the Ag UPD layer (Figure 8a). The experiment of Figure 4 should most directly reflect the height of the produced structure. Place exchange between the Cu surface atoms and the underlying Pt lattice first leads to a surface with Pt atoms at the surface. The effective height differences, if existing at all, are certainly extremely small. However, because the process is taking place in the UPD region, deposition of a monolayer of Cu onto Pt will instantaneously take place, leading to a height difference of theoretically 0.2 nm.

Conclusion

Nanostructuring on Pt single crystal surfaces can be created by tip-induced local alloy formation. Although only simple structures were produced in this work, it is certainly not difficult using an appropriate software for tip positioning also to "write" more complicated structures. It can also be assumed that the method is applicable to other combinations of substrate metal and deposited metal. Certainly, an application of this method to semiconducting surfaces would be interesting.

Although this kind of nanostructuring is possible without using an organic adsorbate as a mask, such a masking adsorbate may be useful in order to achieve nanostructures on a surface which is otherwise free of the UPD metal. In some cases, it may also be possible to desorb the organic adsorbate after this nanolithography. Also, if thicker nanostructured layers are to be produced, such an organic layer may be useful because it blocks the unmodified regions from further deposition, whereas the nanostructured alloy regions are free for further deposition.

A variety of methods for producing organic monolayers on H-terminated Si substrates have been reported.[32] Therefore, this method should also be applicable for use in connection to semiconductor electrodes. As compared to the method of ref 33, it would have the advantage of not only yielding smaller structures but also of being more direct because the processing step of oxide removal by etching is avoided.

Finally, it is quite remarkable that the structure of ethene at electrode surfaces can be imaged at room temperature, whereas in UHV, this adsorbate can only be imaged at low temperatures due to its high mobility. This is similar to the case of adsorbed benzene on Pt: here, imaging in UHV also requires low temperatures or the stabilizing effect of a coadsorbate such as CO,[34,35] whereas at electrode surfaces, it can be imaged at room temperature.[36]

References and Notes

(1) Lebreton, C.; Wang, Z. Z. *Appl. Phys. A: Mater. Sci. Process.* **1998**, *66*, S777−S782.

(2) Park, K. H.; Ha, J. S.; Yun, W. S.; Lee, E. H. *J. Vac. Sci. Technol. A: Vac. Surf. Films* **1999**, *17*, 1441−1444.

(3) Park, K. H.; Ha, J. S.; Yun, W. S.; Ko, Y. J. *Jpn. J. Appl. Phys. Part 1* **2000**, *39*, 4629−4630.

(4) Kolb, D. M.; Engelmann, G. E.; Ziegler, J. C. *Solid State Ionics* **2000**, *131*, 69−78.

(5) Ullmann, R.; Will, T.; Kolb, D. M. *Chem. Phys. Lett.* **1993**, *209*, 239−242.
(6) Engelmann, G. E.; Ziegler, J. C.; Kolb, D. M. *Surf. Sci.* **1998**, *401*, L420−L424.
(7) Ziegler, J. C.; Engelmann, G. E.; Kolb, D. M. *Z. Phys. Chem. Int. J. Res. Phys. Chem. Chem. Phys.* **1999**, *208*, 151−166.
(8) Kolb, D. M.; Ziegler, J. C.; Engelmann, G. E. *Abstr. Papers Am. Chem. Soc.* **2000**, *219*, 467-PHYS.
(9) Schindler, W.; Hofmann, D.; Kirschner, J. *J. Appl. Phys.* **2000**, *87*, 7007−7009.
(10) Hofmann, D.; Schindler, W.; Kirschner, J. *Appl. Phys. Lett.* **1998**, *73*, 3279−3281.
(11) Li, W.; Hsiao, G. S.; Harris, D.; Nyffenegger, R. M.; Virtanen, J. A.; Penner, R. M. *J. Phys. Chem.* **1996**, *100*, 20103−20113.
(12) Lagraff, J. R.; Gewirth, A. A. *J. Phys. Chem.* **1995**, *99*, 10009−10018.
(13) Lagraff, J. R.; Gewirth, A. A. *J. Phys. Chem.* **1994**, *98*, 11246−11250.
(14) Xie, Z.-X.; Kolb, D. M. *J. Electroanal. Chem.* **2000**, *481*, 177−182.
(15) Xiao, X. Y.; Berenz, P.; Baltruschat, H.; Sun, S. *J. Electroanal. Chem.* **2001**, *500*, 446−452.
(16) Chi, Q. J.; Zhang, J. D.; Friis, E. P.; Andersen, J. E. T.; Ulstrup, J. *Surf. Sci.* **2000**, *463*, L641-L648.
(17) Schuster, R.; Kirchner, V.; Allongue, P.; Ertl, G. *Science* **2000**, *289*, 98−101.
(18) Liu, G. Y.; Xu, S.; Qian, Y. L. *Acc. Chem. Res.* **2000**, *33*, 457−466.
(19) Zaera, F. *J. Phys. Chem.* **1990**, *94*, 5090.
(20) Doll, R.; Gerken, C. A.; VanHove, M. A.; Somorjai, G. A. *Surf. Sci.* **1997**, *374*, 151−161.
(21) Janssens, T.; Stone, D.; Hemminger, J.; Zaera, F. *J. Catal.* **1998**, *177*, 284−295.
(22) Pelster, T.; Becker, C.; Tanemura, M.; Breitbach, J.; Wandelt, K. *Surf. Sci.* **1999**, *428*, 398−402.
(23) Land, T. A.; Michely, T.; Behm, R. J.; Hemminger, J. C.; Comsa, G. *J. Chem. Phys.* **1992**, *97*, 6775−6783.
(24) Ronning, M.; Bergene, E.; Borg, A.; Ausen, S.; Holmen, A. *Surf. Sci.* **2001**, *477*, 191−197.
(25) Baltruschat, H. Differential Electrochemical Mass Spectrometry as a Tool for Interfacial Studies. In *Interfacial Electrochemistry*; Wieckowski, A., Ed.; Marcel Dekker: New York, 1999; pp 577−597.
(26) Schmiemann, U.; Baltruschat, H. *J. Electroanal. Chem.* **1992**, *340*, 357.
(27) Schmiemann, U.; Müller, U.; Baltruschat, H. *Electrochim. Acta* **1995**, *40*, 99−107.
(28) Müller, U.; Baltruschat, H. *J. Phys. Chem. B* **2000**, *104*, 5762−5767.
(29) Müller, U.; Dülberg, A.; Baltruschat, H. *Colloids Surf. A* **1998**, *134*, 155−164.
(30) Clavilier, J.; Klein, L. H.; Vaskevich, A.; El-Shafei, A. A. *J. Chem. Soc., Faraday Trans.* **1996**, *92*, 3777−3784.
(31) Bhushan, B. *Wear* **1999**, *225−229*, 465−492.
(32) Boukherroub, R.; Morin, S.; Bensebaa, F.; Wayner, D. D. M. *Langmuir* **1999**, *15*, 3831−3835.
(33) Sugimura, H.; Takai, O.; Nakagiri, N. *J. Electroanal. Chem.* **1999**, *473*, 230−234.
(34) Ogletree, D.; Hofe, M. V.; Somorjai, G. *Surf. Sci.* **1987**, *183*, 1.
(35) Somorjai, G. *J. Phys. Chem.* **1990**, *94*, 1013.
(36) Yau, S. L.; Kim, Y. G.; Itaya, K. *J. Am. Chem. Soc.* **1996**, *118*, 7795−7803.